PHYSICAL REVIEW D **87,** 123541 (2013)

Vector Higgs-portal dark matter and Fermi-LAT gamma ray line

Ki-Young Choi*
Asia Pacific Center for Theoretical Physics and Department of Physics, POSTECH, Pohang, Gyeongbuk 790-784, Republic of Korea

Hyun Min Lee†
School of Physics, KIAS, Seoul 130-722, Republic of Korea

Osamu Seto‡
Department of Life Science and Technology, Hokkai-Gakuen University, Sapporo 062-8605, Japan
(Received 8 April 2013; published 28 June 2013)

We propose a renormalizable model for vector dark matter with extra $U(1)$ gauge symmetry, which is broken by the vacuum expectation value of a complex singlet scalar. When the singlet scalar has a quartic coupling to a heavy charged scalar, the resonance effect enhances the annihilation cross section of vector dark matter into two photons such that a Fermi gamma ray line at about 130 GeV is obtained. In the presence of a tiny mixing between the singlet scalar and the Standard Model Higgs doublet, the relic density is determined dominantly by WW/ZZ and two-photon channels near the resonance pole of the singlet scalar. We also show that various phenomenological bounds coming from the Higgs-to-diphoton decay rate, precision data, and collider searches for the charged scalar and vacuum stability are satisfied in the model.

DOI: 10.1103/PhysRevD.87.123541 PACS numbers: 95.35.+d, 12.60.Cn, 98.70.Vc

I. INTRODUCTION

The existence of dark matter (DM) [1] provides one of the strong motivations to search for physics beyond the Standard Model (SM). Weakly interacting massive particles (WIMPs) have been the promising candidate for dark matter and are assumed to have weak scale interactions with the SM particles and a weak scale mass. However, the property and identity of WIMP dark matter remains unknown and is one of the big puzzles in particle physics and cosmology.

Recently, it has been shown using Fermi-LAT data [2,3] that a gamma ray line spectrum exists at $E_\gamma = 130$ GeV. The signature has been independently confirmed by other groups [4,5] and officially investigated by the Fermi-LAT Collaboration, but with the peak being shifted to $E_\gamma = 135$ GeV [6]. There are some possible explanations such as monoenergetic pulsar winds [7], a Fermi bubble [8,9], or instrumental effects [10–12] including an Earth limb signal [6,13]. The Fermi-LAT Collaboration [14] and the H.E.S.S Collaboration [15] have reported only the upper bound on the annihilation cross section of WIMPs, which is compatible with the Fermi gamma ray line, so the dark matter interpretation of the Fermi-LAT line signature seems plausible.

Dark matter is neutral and thus cannot annihilate into photons at tree level. The generation of photons must happen via the loops of charged particles to which dark matter is directly or indirectly coupled, so the annihilation cross section of dark matter into photons is much suppressed as compared to other tree-level annihilation channels. Thus, in order to realize a large branching fraction of the annihilation cross section into photons, we need to rely on a large coupling to new charged particles running in loops [16–18] or a resonance pole of the mediator particle between dark matter and photons [19,20].

The extra $U(1)$ gauge symmetry is one of the simplest extensions of the SM. In this paper, we propose a renormalizable model of vector dark matter in which the extra $U(1)_X$ gauge boson couples to the SM particles through the mixing between the complex singlet scalar, which is responsible for $U(1)_X$ breakdown, and the SM Higgs doublet. When there is a quartic coupling between the singlet scalar and a heavy charged scalar, dark matter can annihilate into a photon pair with sizable branching fraction, provided that the mixing between the singlet scalar and the SM Higgs boson is small enough. The annihilation cross section of dark matter into a photon pair is enhanced near the resonance pole of the singlet-like scalar mediator to be consistent with a Fermi gamma ray line. For a tiny mixing between the neutral scalars, the thermal relic density can be determined dominantly by annihilation channels into WW, ZZ, and a photon pair. We discuss various phenomenological implications of the model, e.g., Higgs to diphoton rate, electroweak precision measurements, collider constraints on the charged scalar, and the vacuum stability bound of the scalar potential.

We note that in most of the other previous works on vector WIMPs, a vector boson was introduced as a Proca field [21–23] or a scalar sector was described by the

*kiyoung.choi@apctp.org
†hyun.min.lee@kias.re.kr
‡seto@physics.umn.edu

nonlinear sigma model [24]. In our model, vector dark matter is realized as a gauge boson of extra $U(1)$ symmetry when it is broken spontaneously by the vacuum expectation value (VEV) of the hidden Higgs field at the renormalizable level [22,25].

The paper is organized as follows. Beginning with the introduction of our model, in Sec. III, we calculate the annihilation cross section of the $U(1)_X$ gauge boson dark matter and show that the desired thermal relic density and a large annihilation cross section into two monochromatic photons can be realized for a consistent set of parameters. Then, we study the effect of the charged scalar on the Higgs diphoton decay rate in Sec. IV and various experimental constraints on the charged scalar in Sec. V. In Sec. VI, we study the running of the couplings with the modified renormalization group equations (RGEs) due to additional interactions and consequently show how the stability of the Higgs potential is improved. We summarize our results in Sec. VII. There are two appendixes summarizing the gauge and scalar interaction vertices and RG equations, respectively.

II. THE MODEL

We consider a simple model of vector WIMP dark matter that couples to the SM particles through Higgs portal interactions. The gauge sector of the model is based on the $SU(3)_C \times SU(2)_L \times U(1)_Y \times U(1)_X$ gauge group. The extra $U(1)_X$ gauge symmetry is spontaneously broken by the vacuum expectation value (VEV) of a complex scalar S_1. For a minimal extension of the SM,[1] we introduce an $SU(2)$ singlet charged scalar S_2^+, which carries $Y = 1$ but is neutral under $U(1)_X$. We assume that all the SM particles including the Higgs doublet are neutral under the $U(1)_X$.

The model has a Z_2 symmetry under which $S_1 \to S_1^*$ and $X_\mu \to -X_\mu$, which guarantees the stability of vector dark matter X_μ. The Lagrangian of the model is

$$\mathcal{L} = -\frac{1}{4}F_{\mu\nu}F^{\mu\nu} + |D_\mu S_1|^2 + |D_\mu S_2|^2 - V(\Phi, S_1, S_2) + f_{ij}L_i C \cdot L_j S_2^+, \quad (1)$$

where $F_{\mu\nu} = \partial_\mu X_\nu - \partial_\nu X_\mu$, and the covariant derivatives are $D_\mu S_1 = (\partial_\mu - ig_X X_\mu)S_1$ and $D_\mu S_2 = (\partial_\mu - ig' B_\mu)S_2$, with respect to $U(1)_X$ and $U(1)_Y$ gauge symmetry. After the electroweak symmetry breaking, $D_\mu S_2$ is reduced to the covariant derivative with respect to $U(1)_{\rm em}$ symmetry. The scalar potential of the SM Higgs doublet Φ and complex scalar fields S_1 and S_2 is given by

$$V(\Phi, S_1, S_2) = \mu_1^2|\Phi|^2 + \mu_2^2|S_1|^2 + \mu_3^2|S_2|^2 + \frac{1}{2}\lambda_1|\Phi|^4 + \frac{1}{2}\lambda_2|S_1|^4 + \frac{1}{2}\lambda_3|S_2|^4 + \lambda_4|\Phi|^2|S_1|^2 + \lambda_5|\Phi|^2|S_2|^2 + \lambda_6|S_1|^2|S_2|^2. \quad (2)$$

Here the λ_4 coupling is relevant for the mixing between Φ and S_1, after the breaking of $U(1)_X$ and electroweak symmetry. The dominant annihilation of vector dark matter occurs through this coupling so that the correct relic density can be obtained. The coupling λ_6 connects the vector dark matter to the charged particle and enhances the photon emission. The coupling λ_5 in combination of the charged scalar mass can be constrained by the branching ratio of Higgs boson decay into two photons at the Large Hadron Collider (LHC).

In the last term of the Lagrangian (1), L_i is the SM lepton doublet with flavor index $i = 1, 2, 3$, C is the charge-conjugation operator, and the dot denotes the $SU(2)$ antisymmetric product. This term induces the decay of heavy charged scalar $S_2^\pm \to l_i^\pm + \bar{\nu}_j$. The experimental constraints on the lepton flavor violating term will be discussed in Sec V. This model can be extended to a Type-II seesaw model, where the charged scalar S_2 is embedded into a triplet Higgs field with $Y = 2$ [27]. In this case, the lepton couplings of the charged scalar would be small in order to explain neutrino masses.

At the vacuum with a nonvanishing singlet VEV, $\langle S_1 \rangle = v_S/\sqrt{2}$, the $U(1)_X$ gauge symmetry is broken so the gauge boson X_μ acquires mass,

$$M_X^2 = g_X^2 v_S^2. \quad (3)$$

We expand Φ and S_1 fields in unitary gauge, around the electroweak vacuum with $\langle \Phi \rangle = v/\sqrt{2}$ and $\langle S_1 \rangle = v_S/\sqrt{2}$, as

$$\Phi = \begin{pmatrix} 0 \\ \frac{1}{\sqrt{2}}(v + \phi) \end{pmatrix}, \quad (4)$$

$$S_1 = \frac{1}{\sqrt{2}}(v_S + \phi_S), \quad (5)$$

with $v \simeq 246$ GeV. Then, two scalar modes ϕ and ϕ_S in general mix so the mass eigenstates h and H are given in terms of the mixing angle α as

$$h = \cos\alpha\phi - \sin\alpha\phi_S, \quad H = \sin\alpha\phi + \cos\alpha\phi_S. \quad (6)$$

The Higgs mixing essentially depends on λ_4 through

$$\tan 2\alpha = \frac{2\lambda_4 v v_S}{\lambda_1 v^2 - \lambda_2 v_S^2}, \quad (7)$$

and the mass eigenvalues are

[1]The model can be extended with a large multiplet containing a charged scalar such as an extra Higgs doublet or Higgs triplet [26], etc.

$$M^2_{h,H} = \lambda_1 v^2 + \lambda_2 v_S^2 \mp \sqrt{(\lambda_2 v_S^2 - \lambda_1 v^2)^2 + 4\lambda_4^2 v^2 v_S^2}. \tag{8}$$

For a small mixing angle α, we can regard $h \simeq \phi$ as being SM Higgs-like, $H \simeq \phi_S$ as being singletlike, and the mass eigenvalues are $M_h \simeq \lambda_1 v^2$ and $M_H^2 \simeq \lambda_2 v_S^2$. The gauge and scalar interactions of the Higgs fields are listed in Appendix A.

The absolute stability of the electroweak vacuum gives rise to the following conditions on the quartic couplings in the scalar potential [28],

$$\begin{aligned} &\lambda_1 > 0, \qquad \lambda_2 > 0, \qquad \lambda_3 > 0, \\ &\lambda_{12} \equiv \lambda_4 + \sqrt{\lambda_1 \lambda_2} > 0, \\ &\lambda_{13} \equiv \lambda_5 + \sqrt{\lambda_1 \lambda_3} > 0, \\ &\lambda_{23} \equiv \lambda_6 + \sqrt{\lambda_2 \lambda_3} > 0, \end{aligned} \tag{9}$$

and

$$\begin{aligned} \lambda_{123} \equiv \frac{1}{2}\sqrt{\lambda_1 \lambda_2 \lambda_3} + \lambda_6 \sqrt{\lambda_1} + \lambda_5 \sqrt{\lambda_2} + \lambda_4 \sqrt{\lambda_3} \\ + \sqrt{\lambda_{12} \lambda_{23} \lambda_{13}} > 0. \end{aligned} \tag{10}$$

Throughout this paper, we also impose perturbativity conditions until the Planck scale as

$$|\lambda_i| < 4\pi. \tag{11}$$

III. RELIC DENSITY AND FERMI GAMMA RAY LINES

In this section, we compute the DM annihilation cross sections and discuss the constraints of the relic density and the Fermi gamma ray line in the model.

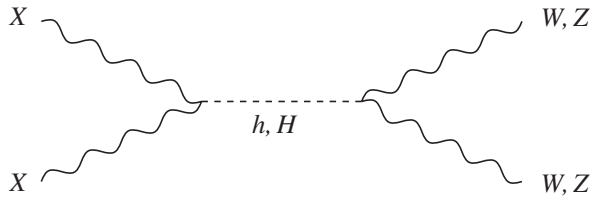

FIG. 1. Feynman diagram for annihilations of vector dark matter into WW, ZZ at tree level.

A. Thermal relic abundance

The thermal relic abundance of the vector WIMP dark matter X is estimated by integrating the following Boltzmann equation for the dark matter number density n_X in the early Universe [29,30],

$$\frac{dn_X}{dt} + 3Hn_X = -\langle \sigma v \rangle (n_X^2 - (n_X^{\rm EQ})^2), \tag{12}$$

where H, $\langle \sigma v \rangle$, and $n_X^{\rm EQ}$ denote the Hubble parameter, the thermal-averaged annihilation cross section times relative velocity, and the dark matter number density at thermal equilibrium, respectively. X dominantly annihilates into W and Z boson pairs through the s-channel exchange of the Higgs bosons h and H, as shown in Fig. 1. The magnitude of those annihilation cross sections is proportional to $(\sin\alpha \cos\alpha)^2$ and thus scaled by the mixing angle between Higgs bosons. A larger (smaller) annihilation cross section is realized for a larger (smaller) $\sin\alpha$. The velocity times DM annihilation cross sections into W, Z boson pairs before thermal average are given by

$$\begin{aligned} (\sigma v)_{WW}(s) = \frac{1}{18\pi s} \left| \frac{g_{XXh} g_{hWW}}{s - M_h^2 + iM_h\Gamma_h} + \frac{g_{XXH} g_{HWW}}{s - M_H^2 + iM_H\Gamma_H} \right|^2 \\ \times \left\{ 1 + \frac{1}{2M_X^4} \left(\frac{s}{2} - M_X^2 \right)^2 \right\} \left\{ 1 + \frac{1}{2M_W^4} \left(\frac{s}{2} - M_W^2 \right)^2 \right\} \sqrt{1 - \frac{4M_W^2}{s}}, \end{aligned} \tag{13}$$

and

$$\begin{aligned} (\sigma v)_{ZZ}(s) = \frac{1}{36\pi s} \left| \frac{g_{XXh} g_{hZZ}}{s - M_h^2 + iM_h\Gamma_h} + \frac{g_{XXH} g_{HZZ}}{s - M_H^2 + iM_H\Gamma_H} \right|^2 \\ \times \left\{ 1 + \frac{1}{2M_X^4} \left(\frac{s}{2} - M_X^2 \right)^2 \right\} \left\{ 1 + \frac{1}{2M_Z^4} \left(\frac{s}{2} - M_Z^2 \right)^2 \right\} \sqrt{1 - \frac{4M_Z^2}{s}}, \end{aligned} \tag{14}$$

where s is the total energy at the center of mass frame and the couplings are given by

$$\begin{aligned} &g_{XXh} = -2g_X^2 v_S \sin\alpha, \qquad g_{XXH} = 2g_X^2 v_S \cos\alpha, \qquad g_{hWW} = \frac{1}{2} g_2^2 v \cos\alpha, \\ &g_{HWW} = \frac{1}{2} g_2^2 v \sin\alpha, \qquad g_{hZZ} = \frac{g_2^2}{2\cos\theta_W^2} v \cos\alpha, \qquad g_{HZZ} = \frac{g_2^2}{2\cos\theta_W^2} v \sin\alpha. \end{aligned} \tag{15}$$

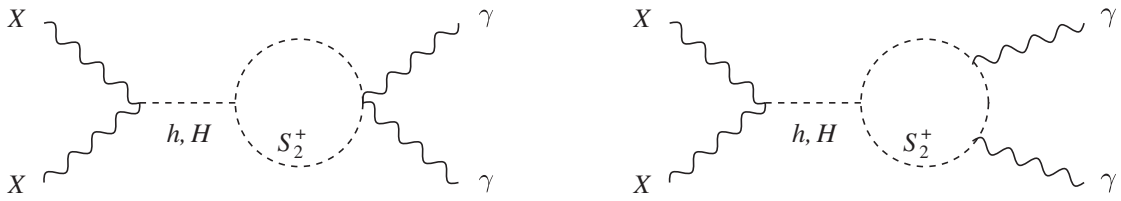

FIG. 2. Feynman diagrams for the annihilation of vector dark matter into a photon pair at one loop.

Moreover, the corresponding expression for the DM annihilation into hh is also given by

$$(\sigma v)_{hh}(s) = \frac{1}{72\pi s}\left|\frac{g_{XXh}g_{hhh}}{s - M_h^2 + iM_h\Gamma_h} + \frac{g_{XXH}g_{Hhh}}{s - M_H^2 + iM_H\Gamma_H}\right|^2\left\{1 + \frac{1}{2M_X^4}\left(\frac{s}{2} - M_X^2\right)^2\right\}\sqrt{1 - \frac{4M_h^2}{s}}, \tag{16}$$

where

$$g_{hhh} = 3v(\lambda_1\cos^3\alpha + \lambda_4\sin^2\alpha\cos\alpha) - 3v_S(\lambda_2\sin^3\alpha + \lambda_4\sin\alpha\cos^2\alpha), \tag{17}$$

$$g_{Hhh} = \frac{1}{4}v(\sin\alpha(3\lambda_1 + \lambda_4) + 3\sin 3\alpha(\lambda_1 - \lambda_4)) + \frac{1}{4}v_S(\cos\alpha(3\lambda_2 + \lambda_4) + 3\cos 3\alpha(\lambda_4 - \lambda_2)). \tag{18}$$

However, we find that the annihilation cross section of the hh channel is numerically smaller than those of the WW, ZZ channels by an order of magnitude, which has the polarization sum over the final states. The other annihilation channels with hH and HH final states are kinematically forbidden near the resonance, $M_H \sim 2M_X$.

Finally, when there is a sizable quartic coupling between the singlet scalar and the heavy charged scalar S_2, dark matter can annihilate into a photon pair, due to loops with the charged scalar S_2^+ as shown in Fig. 2. The velocity times DM annihilation cross section into a photon pair before thermal average is expressed by

$$(\sigma v)_{\gamma\gamma}(s) = \frac{\alpha_{\rm em}^2}{96\pi^3 s}\left|\sum_{H_i=h,H}\frac{g_{XXH_i}g_{H_iS_2^+S_2^-}}{s - M_{H_i}^2 + iM_{H_i}\Gamma_{H_i}}\right|^2\left|1 - \frac{M_{S_2^+}^2}{M_X^2}f\left(\frac{M_{S_2^+}^2}{M_X^2}\right)\right|^2\left\{1 + \frac{1}{2M_X^4}\left(\frac{s}{2} - M_X^2\right)^2\right\}, \tag{19}$$

with

$$f(\tau) = [\sin^{-1}(1/\sqrt{\tau})]^2. \tag{20}$$

Depending on the mixing angle α, the DM annihilation into a photon pair can have a sizable branching fraction, as will be illustrated in the later subsection.

The heavy Higgs boson mainly decays into XX, and also into W, Z, and h pairs suppressed by the mixing. The decay width is given by

$$\begin{aligned}\Gamma_H = {} & \frac{M_H^3\sin^2\alpha}{32\pi v^2}\left[2\left(1 - \frac{4M_W^2}{M_H^2} + \frac{12M_W^4}{M_H^4}\right)\sqrt{1 - \frac{4M_W^2}{M_H^2}} + \left(1 - \frac{4M_Z^2}{M_H^2} + \frac{12M_Z^4}{M_H^4}\right)\sqrt{1 - \frac{4M_Z^2}{M_H^2}}\right] \\ & + \frac{M_H^3\cos^2\alpha}{32\pi v_S^2}\left(1 - \frac{4M_X^2}{M_H^2} + \frac{12M_X^4}{M_H^4}\right)\sqrt{1 - \frac{4M_X^2}{M_H^2}} + \frac{g_{Hhh}^2}{8\pi M_H}\sqrt{1 - \frac{4M_h^2}{M_H^2}} + \Gamma(H \to S_2S_2^* \to S_2 l\nu).\end{aligned} \tag{21}$$

Here, the three-body decay mode with one charged scalar S_2 being off-shell can be ignored when the lepton couplings to the charged scalar is small enough. We assume that this is the case, due to precision constraints associated with leptons as will be discussed in the later section.

We are interested in the case where X has a large annihilation cross section into two photons so that the gamma ray line at 135 GeV observed by Fermi LAT can be explained. Taking the annihilation into a W or Z boson pair through h and H exchange to be strongly suppressed due to a tiny mixing angle between SM Higgs boson and singlet scalars, namely, $|\sin\alpha| \ll 1$, we obtain the desired thermal relic density and the necessary cross section into a photon pair for Fermi gamma ray line near the resonance pole of the singlet-like scalar [19,20]. The necessary tiny mixing between the neutral scalars is given by $\lambda_4 \sim \frac{1}{8\pi^2}\lambda_5\lambda_6\ln(M_{S_2^\pm}/\mu)$ from the one-loop corrections of the charged scalar S_2, provided that the tree-level mixing vanishes.[2] For instance,

[2]One of the possibilities to realize a vanishing λ_4 at tree level is to put the model into extra dimensions. Namely, the charged scalar S_2 lives in the bulk of extra dimensions, while vector dark matter and S_1 are localized on a different location in extra dimensions compared with the Higgs doublet.

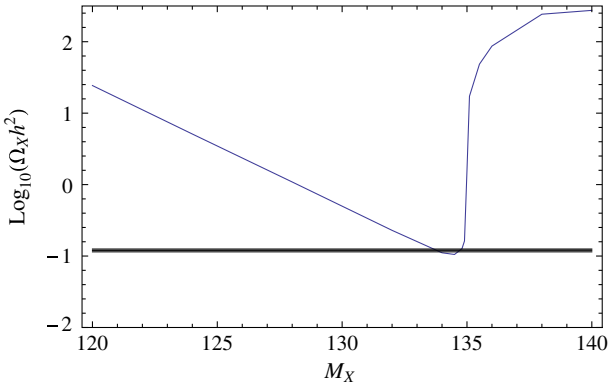

FIG. 3 (color online). The plot of relic density of the dark matter Ωh^2 vs its mass. Here we used $M_{S_2^\pm} = 140$ GeV, $v_S = 1$ TeV, $\sin\alpha = 0.00047$, and $\lambda_6 = 0.2$. We can ignore the λ_5 dependence for the parameter region in our interest. The horizontal line is the relic density of cold dark matter revealed by the Planck result, $\Omega_{\mathrm{CDM}} h^2 = 0.1199 \pm 0.0027$ [53].

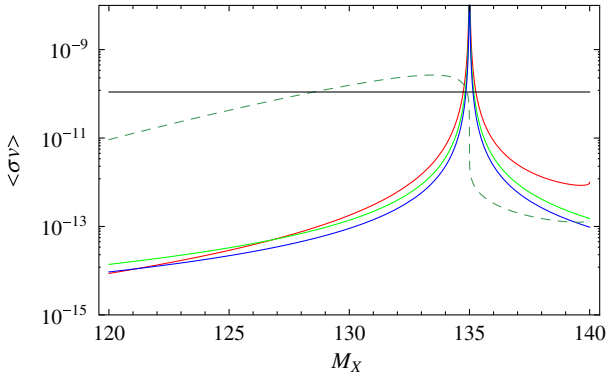

FIG. 4 (color online). Thermal-averaged annihilation cross section (dashed line), given by the sum of $\gamma\gamma$, WW, ZZ final states at the freeze-out temperature of dark matter, $T_f = M_X/20$. Solid lines are at zero temperature (red: $\gamma\gamma$, blue: WW, green: ZZ final states). Here we used the same parameters in Fig. 3. The horizontal black line is the value of the DM annihilation cross section into two photons, $\langle\sigma v\rangle_{\chi\chi\to\gamma\gamma} = 1.1 \times 10^{-10}$ GeV^{-2}, needed for the Fermi-LAT gamma ray line.

for $\lambda_5 \sim \lambda_6 \sim 0.1$, we can get $|\lambda_4| \sim 10^{-4}$, which is desirable for explaining both the relic density and Fermi gamma ray line as will be shown later. Therefore, near the resonance, $M_X \simeq M_H/2$, for the WIMP mass[3] around 135 GeV, we need to take the singlet-scalar mass M_H to be about 270 GeV.

In Fig. 3, we show that the right relic density of WIMPs can be obtained by performing the thermal average of the annihilation cross section for all the dominant channels, with the procedure in Ref. [30]. We note that there is no bound on vector dark matter from direct detection in our model, due to a tiny Higgs mixing.

B. Monochromatic photons from DM annihilation

Now we discuss the aspect of the indirect detection of vector WIMPs. In addition to the WW/ZZ annihilation channels, X can also annihilate into two monochromatic photons with the effective interaction induced by the heavy charged scalar. Hence, this diphoton mode can provide a source for the gamma ray line observed by Fermi LAT. When the singlet-like scalar H has small couplings to W and Z bosons due to a tiny $\sin\alpha$ but it has a sizable coupling to the charged scalar S_2, the diphoton mode takes a larger branching fraction of the annihilation cross section than usually expected.

Keeping only the H-exchange contribution in Eq. (19) for a small Higgs mixing and using $s \simeq 4M_X^2$, we get an approximate form for the thermal-averaged annihilation cross section into a photon pair at present as

$$\langle\sigma v\rangle_{\gamma\gamma} \simeq \frac{\alpha_{\mathrm{em}}^2}{96\pi^3 M_X^2}\left|\frac{\lambda_6 \cos^2\alpha M_X^2}{4M_X^2 - M_H^2 + iM_H\Gamma_H}\right|^2 \times \left|1 - \frac{M_{S_2^+}^2}{M_X^2} f\left(\frac{M_{S_2^+}^2}{M_X^2}\right)\right|^2. \quad (22)$$

In Fig. 4, we show, as a function of the DM mass, the annihilation cross sections into WW, ZZ, $\gamma\gamma$ at zero temperature, and the thermal averaged total annihilation cross section used to estimate Ωh^2, respectively. To explain the gamma ray line spectrum of the Fermi-LAT [2,3] for the Einasto dark matter profile, we require that

$$\langle\sigma v\rangle_{\chi\chi\to\gamma\gamma} = (1.27 \pm 0.32^{+0.18}_{-0.28}) \times 10^{-27}\ \mathrm{cm}^3\,\mathrm{s}^{-1}, \approx 1.1 \times 10^{-10}\ \mathrm{GeV}^{-2}. \quad (23)$$

In order to obtain the observed Fermi gamma ray line together with the correct relic density, the small mixing angle, $|\sin\alpha| \ll 1$, is necessary. Furthermore, the annihilation into WW and ZZ modes have to be suppressed enough not to generate too many continuum photons [31–33]. In our case, the DM annihilation cross sections into WW and ZZ are suppressed at present for the parameters, which explains both the Fermi gamma ray line and the relic density. For instance, for $M_X = 134.74$ GeV, we obtain $\langle\sigma v\rangle_{\gamma\gamma} = 1.09 \times 10^{-10}$ GeV^{-2} and $\Omega h^2 = 0.118$ while $\langle\sigma v\rangle_{ZZ}/\langle\sigma v\rangle_{\gamma\gamma} = 0.43$ and $\langle\sigma v\rangle_{WW}/\langle\sigma v\rangle_{\gamma\gamma} = 0.28$. We note that the total DM annihilation cross section at present is smaller than thermal cross section, because the temperature effect shifts the peak of the resonance at freeze-out towards a smaller DM mass as compared to the case with zero temperature [34].

The same diagrams in Fig. 2 apply to the annihilation of vector dark matter into $Z\gamma$ and loop-induced ZZ final

[3]Of course, there is another resonance region $M_X \simeq M_h/2 \simeq 63$ GeV, where the main annihilation mode is $XX \to b\bar{b}$.

states. The annihilation $XX \to Z\gamma$ emits an additional gamma line at $E_\gamma = 114$ GeV, and the resulting flux is suppressed by 0.21 as compared to that of 130 GeV gamma ray line [17], while the loop-induced annihilation into ZZ is negligible.

IV. HIGGS TO DIPHOTON RATE

The charged scalar S_2, introduced to explain the Fermi gamma ray line, can give a positive or negative sizable contribution to the Higgs-to-diphoton rate[4] due to the quartic coupling λ_5 to the SM Higgs field. In this section, we discuss the constraint on the modified decay rate of Higgs boson h to diphotons from the recent measurements at the LHC.

We define the ratio of the Higgs production cross section times the branching fraction, $\mu_{\gamma\gamma} \equiv \frac{\sigma \times \mathrm{Br}_{\gamma\gamma}}{(\sigma \times \mathrm{Br}_{\gamma\gamma})_{SM}}$. The reported signal strengths for the Higgs to diphoton rate from ATLAS and multivariate analysis of CMS data are the following [36]:

$$\mu_{\gamma\gamma}^{\mathrm{ATLAS}} = 1.65^{+0.34}_{-0.30}, \qquad \mu_{\gamma\gamma}^{\mathrm{CMS}} = 0.78^{+0.28}_{-0.26}. \tag{24}$$

Following a similar method as in Refs. [37,38] and assuming that the combined data is Gaussian, we have derived the combined value of the Higgs to diphoton rate as

$$\mu_{\gamma\gamma}^{\mathrm{combi}} = 1.18 \pm 0.20. \tag{25}$$

The SM-like Higgs boson decay width $\Gamma(h \to \gamma\gamma)$ is given by [39]

$$\Gamma(h \to \gamma\gamma) = \frac{G_F \alpha^2 M_h^3}{128\sqrt{2}\pi^3} |g_W A_1(\tau_W) + g_t Q_t^2 N_c A_{1/2}(\tau_t) + g_h A_0(\tau_{S_2^\pm})|^2, \tag{26}$$

with loop functions

$$A_1(x) = -x^2[2x^{-2} + 3x^{-1} + 3(2x^{-1} - 1)f(x^{-1})], \tag{27}$$

$$A_{1/2}(x) = 2x^2[x^{-1} + (x^{-1} - 1)f(x^{-1})], \tag{28}$$

$$A_0(x) = -x^2[x^{-1} - f(x^{-1})], \tag{29}$$

$$f(x) = \begin{cases} \arcsin^2\sqrt{x} & \text{for } x \le 1 \\ -\frac{1}{4}\left(\ln\left(\left(1 + \sqrt{1 - x^{-1}}\right)\Big/\left(1 + \sqrt{1 - x^{-1}}\right)\right) - i\pi\right)^2 & \text{for } x > 1, \end{cases} \tag{30}$$

and $\tau_i = 4M_i^2/M_h^2$. $Q_t = \frac{2}{3}$, $N_c = 3$ for top quark. g_W and g_t are the Higgs trilinear couplings to the W gauge boson and top quark normalized to the ones of the SM, and in our case those are almost 1. The Higgs coupling to the charged scalar boson is

$$g_h = \frac{M_W}{g M_{S_2^\pm}^2} v \lambda_5. \tag{31}$$

By taking the ratio to the SM value, we obtain

$$R_{\gamma\gamma} \equiv \frac{\Gamma(h \to \gamma\gamma)}{\Gamma(h \to \gamma\gamma)_{\mathrm{SM}}} = \left| 1 + \frac{g_h A_0(\tau_{S_2^\pm})}{g_W A_1(\tau_W) + g_t Q_t^2 N_c A_{1/2}(\tau_t)} \right|^2, \tag{32}$$

which is a function of λ_5 and $M_{S_2^\pm}$. When the production cross section of h is SM Higgs-like, the above ratio is approximated to the signal strength measured at the LHC, that is, $R_{\gamma\gamma} \simeq \mu_{\gamma\gamma}$.

[4]A similar discussion on the role of charged matter can be also found in the context of a scalar dark matter in Ref. [35].

In Fig. 5, we depict the parameter space $(\lambda_5, M_{S_2^\pm})$, showing the contours of the h decay to diphoton rate with other Higgs couplings being assumed the same as in the SM. We find that, from the combined value of ATLAS and CMS (multivariate analysis) diphoton signal strengths at 90% C.L., the extra quartic coupling is constrained to $-2.5 \lesssim \lambda_5 \lesssim 0.7$ for $M_{S_2^\pm} = 140$ GeV. The heavier the charged scalar, the larger the values of the extra quartic coupling λ_5 that are allowed.

V. CONSTRAINTS ON CHARGED SCALAR

We have introduced the lepton couplings to the charged scalar S_2 by gauge-invariant terms, $f_{ij} L_i^c \cdot L_j S_2$, so S_2 could be unstable. In this section, we discuss the phenomenology of the charged scalar from the indirect limits and the collider search for charged particles at the LHC.

The lepton couplings to the charged scalar are similar to lepton number (R-parity) violating terms in the minimal supersymmetric standard model, $\Delta W = \lambda_{ijk} L_i \cdot L_j E_k^c$, so the same bounds from precision measurements are applied to them. The bounds from the charged current universality are $|f_{12}| < 0.04(M_{S_2^\pm}/(100\ \mathrm{GeV}))$, and the constraints

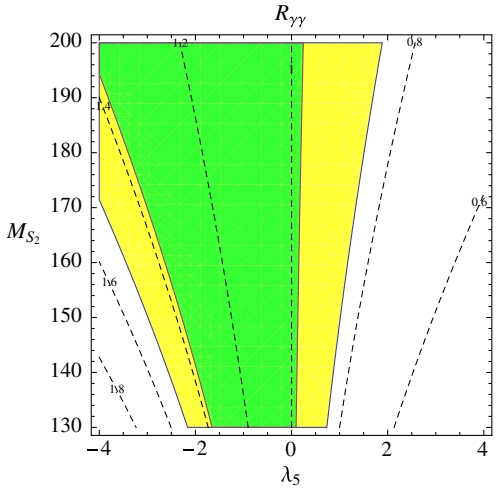

FIG. 5 (color online). Contours of Higgs to diphoton rate on $\lambda_5 - M_{S_2^\pm}$ plane. The green and yellow regions correspond to the combined LHC bounds on $R_{\gamma\gamma}$ at 68% and 90% C. L., respectively.

from $R_\tau = \Gamma(\tau \to e\nu\bar{\nu})/\Gamma(\tau \to \mu\nu\bar{\nu})$ or $R_{\tau\mu} = \Gamma(\tau \to \mu\nu\bar{\nu})/\Gamma(\mu \to e\nu\bar{\nu})$ are $|f_{ij}| < 0.05(M_{S_2^\pm}/(100\ \text{GeV}))$, and ν_μ deep inelastic scattering gives the bound, $|f_{12}| < 0.02(M_{S_2^\pm}/(100\ \text{GeV}))$ [40]. Other lepton flavor violation $\text{Br}(\mu \to e\gamma)$ also gives a similar bounds [41]. The charged scalar couplings contribute to the effective tree-level Fermi coupling in μ decay by $G_\mu/\sqrt{2} = g^2/(8M_W^2) + |f_{12}|^2/(8M_{S_2^\pm}^2)$, but they give a less stringent limit than the bounds quoted above [42]. The lepton Yukawa couplings gives a negative contribution[5] to the muon anomalous magnetic moment as [43,44]

$$\Delta a_\mu = -\frac{m_\mu^2}{96\pi^2}\frac{1}{M_{S_2^\pm}^2}(|f_{12}|^2 + |f_{23}|^2). \tag{33}$$

Then, using the bounds from precision measurements, we get a very small contribution, $|\Delta a_\mu| < 3.45 \times 10^{-12}$. We note that as far as the electroweak precision bounds on f_{ij} are satisfied for $M_{S_2^\pm} \gtrsim 130$ GeV, the continuum photons coming from the three-body DM annihilation into $S_2 l\nu$ can be suppressed enough.

New particles with electroweak charges have been searched for at colliders. The stringent bounds on the charged scalar come from the direct slepton pair production at the LHC [45,46], where a left-handed slepton can decay into lepton and neutralino. The opposite-sign dilepton search with the same-flavor channel at CMS excludes slepton masses between 110 and 275 GeV for massless neutralino [46]. But, in our case, the charged scalar can decay into all the charged leptons: $S_2^- \to e\bar{\nu}_{\mu,\tau}$, $\mu\bar{\nu}_{e,\tau}$, and $\tau\bar{\nu}_{e,\mu}$. Since the lepton coupling matrix, f_{ij}, is antisymmetric, at least two different flavors always appear in the decay product of the charged scalar. Therefore, the CMS mass limit with the same-flavor channel scales down or does not apply, depending on the branching fraction of the same-flavor decay mode. Currently, the most stringent constraint on the charged scalar mass comes from the LEP exclusion limit up to 95 GeV [47].

VI. VACUUM STABILITY

The discovered scalar boson with 126 GeV mass has been shown to have very similar properties to the SM Higgs boson with more precision [48]. Although we need more data to confirm the properties of the Higgs boson, we assume that the discovered scalar boson is SM Higgs-like. In this case, a small Higgs quartic coupling leads to a problem of vacuum instability below the Planck scale [49], requiring new physics beyond the SM.[6] In this section, we discuss the effect of the additional quartic couplings between the Higgs boson and extra scalars in the model, taking account of dark matter constraints from Fermi gamma ray line, Higgs boson data and other collider bounds, discussed in the previous sections.

In our model, it is possible to have a sizable shift in the Higgs quartic coupling in the presence of the mixing with a singlet scalar [50–52] as follows,

$$\lambda_{\text{eff}} = \lambda_1 - \delta\lambda, \tag{34}$$

with

$$\delta\lambda = \frac{(M_H^2 - M_h^2)^2 \sin^2\alpha \cos^2\alpha}{v^2(M_H^2\cos^2\alpha + M_h^2\sin^2\alpha)}. \tag{35}$$

In the decoupling limit of a heavy singletlike scalar with $M_H \gg M_h$, the tree-level shift is approximated to $\delta\lambda \simeq M_H^2 \sin^2\alpha/(v^2) \simeq \lambda_4^2/\lambda_2$ [50,51]. In this paper, however, we take the singletlike scalar mass to be close to the resonance pole, $M_H \sim 2M_X \sim 270$ GeV. Furthermore, since $|\sin\alpha| \ll 1$ for the correct relic density at the resonance, the tree-level shift in our case becomes $\delta\lambda \simeq 0.7\sin^2\alpha$, which is extremely small.

Now we consider the RG effect on the Higgs quartic coupling. As shown in Appendix B, there are positive contributions to the beta function of the Higgs quartic coupling, λ_4 and λ_5, in the RG equations, so the vacuum stability can be improved as compared to the SM. But, from the results of the previous sections, the quartic coupling λ_4 between the Higgs doublet and the singlet scalar must be small because of the relic density condition, hence its contribution to the running of the Higgs quartic

[5]There was an error in the previous works on the LLS_2 coupling [41], which showed a positive contribution to the muon anomalous magnetic moment.

[6]We note that when the top pole mass is smaller than 171 GeV, the electroweak vacuum could be absolutely stable until the Planck scale without new physics [49,50].

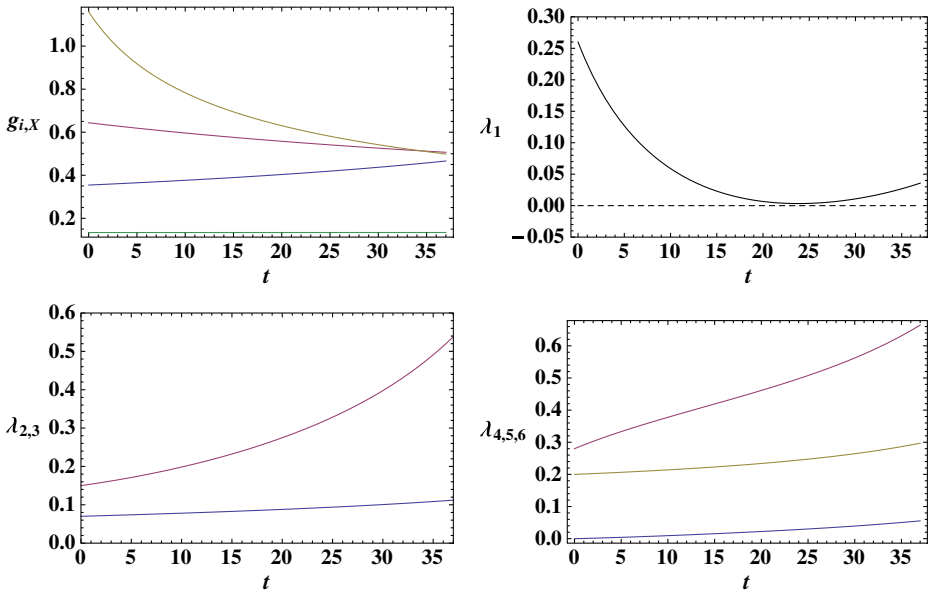

FIG. 6 (color online). Running couplings as a function of $t = \ln(\mu/M_t)$. We have chosen $\lambda_1 = 0.26$, $\lambda_2 = 0.07$, $\lambda_3 = 0.15$, $\lambda_4 = -0.0001$, $\lambda_5 = 0.28$, $\lambda_6 = 0.2$ and $g_X = 0.134$ at the top pole mass, $M_t = 173$ GeV, which leads to $M_X = 134$, $M_H = 270$, $M_h = 126$ GeV and $\sin\alpha = 0.0005$ with $v_S = 1$ TeV. The lepton couplings to the charged scalar are ignored in the RG analysis.

coupling is negligible. On the other hand, a sizable quartic coupling λ_5 between the Higgs doublet and the charged scalar is allowed, being consistent with the observed Higgs boson decay rate to diphoton.

If λ_5 is positive, it can help increase the vacuum instability scale, without violating the new vacuum stability conditions of extra scalars. We note, however, that if λ_5 is negative and large as suggested by Higgs data, it could increase the Higgs quartic coupling by the RG further, but perturbativity bound and extra vacuum stability conditions strongly restrict this possibility. In Fig. 6, we show the running couplings until the Planck scale for the low-energy couplings including a positive λ_5, which are consistent with the Fermi gamma ray line, relic density, Higgs diphoton data, and indirect and collider bounds. In Fig. 7, the vacuum stability conditions are shown to be satisfied until the Planck scale, for the same parameters as in Fig. 6.

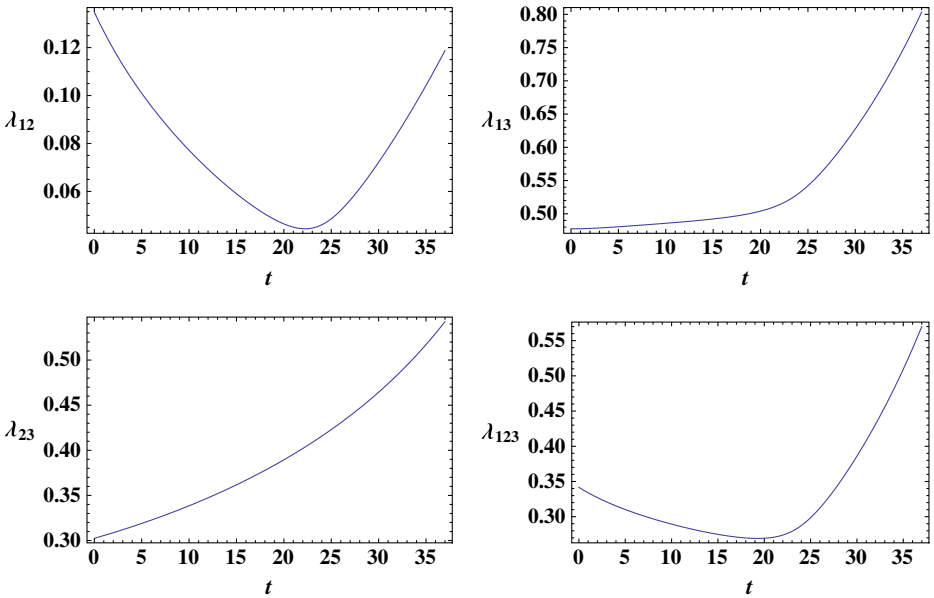

FIG. 7 (color online). Vacuum stability conditions: $\lambda_{12} > 0$, $\lambda_{13} > 0$, $\lambda_{23} > 0$ and $\lambda_{123} > 0$. The same parameters are chosen as in Fig. 6.

VII. CONCLUSION

We have proposed a renormalizable model of vector dark matter, where the extra $U(1)_X$ gauge boson is a dark matter candidate and interacts with the SM particles through the Higgs portal term, namely, the mixing between the $U(1)_X$ breaking singlet scalar and the SM Higgs doublet. If the Higgs mixing is small enough, the DM annihilations into W and Z boson pairs at the resonance pole of the singletlike scalar can reproduce the correct thermal relic density without overproducing continuum photons. In the presence of a quartic coupling between the singlet scalar and the charged scalar S_2, vector dark matter also annihilates into a photon pair with a sizable branching fraction at the same singlet resonance.

As long as the couplings of the charged scalar to the SM leptons are small enough, i.e., $f_{ij} < \mathcal{O}(10^{-2})$, we showed that all the electroweak precision constraints concerning leptons are satisfied. Even though it would be very difficult to find the singlet scalar at colliders due to a tiny mixing with the Higgs, the charged scalar would be accessible at the LHC or linear colliders, due to a distinct signature that two opposite-sign leptons of different flavors are equally produced from the charged scalar decay. We have also shown that the vacuum stability bounds are satisfied until the Planck scale, due to a sizable Higgs coupling to the charged scalar, which is allowed by the current Higgs diphoton data.

ACKNOWLEDGMENTS

K.-Y. C was supported by the Basic Science Research Program through the National Research Foundation of Korea (NRF) funded by the Ministry of Education, Science and Technology (No. 2011-0011083). K.-Y. C acknowledges the Max Planck Society (MPG), the Korea Ministry of Education, Science and Technology (MEST), Gyeongsangbuk-Do, and Pohang City for the support of the Independent Junior Research Group at the Asia Pacific Center for Theoretical Physics (APCTP). The work of O. S. is supported in part by scientific research grants from Hokkai-Gakuen. O. S. thanks the Physik Department T30d, Technische Universitat Munchen for its warm hospitality during his visit supported by the Japan Society for the Promotion of Science and Deutscher Akademischer Austauschdienst, where this work has been completed.

APPENDIX A: SCALAR INTERACTION VERTICES

Gauge interactions:

$$\mathcal{L}_{\rm int} = g_X^2 X^2 v_S (H\cos\alpha - h\sin\alpha) + \frac{g_2^2}{4c_W^2}(2c_W^2 W^- W^+ + Z^2) v (h\cos\alpha + H\sin\alpha). \tag{A1}$$

Scalar interactions:

$$\begin{aligned}
-\mathcal{L}_{\rm int} =& \frac{1}{2}(v\lambda_1\cos^3\alpha + v\lambda_4\sin^2\alpha\cos\alpha - v_S\lambda_2\sin^3\alpha - v_S\lambda_4\sin\alpha\cos^2\alpha)h^3 + \frac{1}{8}(v\sin\alpha(3\lambda_1+\lambda_4) \\
&+ 3v\sin 3\alpha(\lambda_1-\lambda_4) + v_S\cos\alpha(3\lambda_2+\lambda_4) + 3v_S\cos 3\alpha(\lambda_4-\lambda_2))h^2H + \frac{1}{8}(v\cos\alpha(3\lambda_1+\lambda_4) \\
&- 3v\cos 3\alpha(\lambda_1-\lambda_4) - v_S\sin\alpha(3\lambda_2+\lambda_4) + 3v_S\sin 3\alpha(\lambda_4-\lambda_2))hH^2 + \frac{1}{2}(v\lambda_1\sin^3\alpha + v\lambda_4\sin\alpha\cos^2\alpha \\
&+ v_S\lambda_2\cos^3\alpha + v_S\lambda_4\cos\alpha\sin^2\alpha)H^3 + (v\lambda_5\cos\alpha - v_S\lambda_6\sin\alpha)hS^+S^- + (v\lambda_5\sin\alpha + v_S\lambda_6\cos\alpha)HS^+S^- \\
&+ \frac{1}{8}(\cos^4\alpha\lambda_1 + \sin^4\alpha\lambda_2 + 2\cos^2\alpha\sin^2\alpha\lambda_4)h^4 + \frac{1}{8}(\sin^4\alpha\lambda_1 + \cos^4\alpha\lambda_2 + 2\cos^2\alpha\sin^2\alpha\lambda_4)H^4 \\
&+ \frac{1}{2}(\cos^3\alpha\sin\alpha(\lambda_1-\lambda_4) - \cos\alpha\sin^3\alpha(\lambda_2-\lambda_4))h^3H + \frac{1}{2}(\cos\alpha\sin^3\alpha(\lambda_1-\lambda_4) - \cos^3\alpha\sin\alpha(\lambda_2-\lambda_4))hH^3 \\
&+ \frac{1}{4}((\cos^4\alpha - 4\cos^2\alpha\sin^2\alpha + \sin^4\alpha)\lambda_4 + 3\cos^2\alpha\sin^2\alpha(\lambda_1+\lambda_2))h^2H^2 + \frac{1}{2}(\cos^2\alpha\lambda_5 + \sin^2\alpha\lambda_6)h^2S^+S^- \\
&+ \frac{1}{2}(\sin^2\alpha\lambda_5 + \cos^2\alpha\lambda_6)H^2S^+S^- + \sin\alpha\cos\alpha(\lambda_5-\lambda_6)hHS^+S^- + \frac{1}{2}\lambda_3|S^+S^-|^2.
\end{aligned} \tag{A2}$$

APPENDIX B: RENORMALIZATION GROUP EQUATIONS

The running of the coupling p_i is governed by the RG equation, $\frac{\partial p_i}{\partial t} = \beta_{p_i}$, with β_{p_i} being the corresponding beta function and $t \equiv \ln(\mu/m_t)$. The beta functions for scalar quartic couplings with $\kappa \equiv 16\pi^2$ are

$$\kappa\beta_{\lambda_1} = 12\lambda_1^2 + (12y_t^2 - 9g^2 - 3g'^2)\lambda_1 - 12y_t^4 + \frac{9}{4}g^4 + \frac{3}{4}g'^4 + \frac{3}{2}g^2g'^2 + 2\lambda_4^2 + 2\lambda_5^2, \tag{B1}$$

$$\kappa\beta_{\lambda_2} = 10\lambda_2^2 + 4\lambda_4^2 + 2\lambda_6^2 - 12g_X^2\lambda_2 + 12g_X^4, \tag{B2}$$

$$\kappa\beta_{\lambda_3} = 10\lambda_3^2 + 4\lambda_5^2 + 2\lambda_6^2 + (4\,\mathrm{Tr}(f^\dagger f) - 12g'^2)\lambda_3 + 12g'^4 - 4\,\mathrm{Tr}(ff^\dagger ff^\dagger), \tag{B3}$$

$$\kappa\beta_{\lambda_4} = (6\lambda_1 + 4\lambda_2 + 4\lambda_4)\lambda_4 + 2\lambda_5\lambda_6 + \left(6y_t^2 - \frac{3}{2}g'^2 - \frac{9}{2}g^2 - 6g_X^2\right)\lambda_4, \tag{B4}$$

$$\kappa\beta_{\lambda_5} = (6\lambda_1 + 4\lambda_3 + 4\lambda_5)\lambda_5 + 2\lambda_4\lambda_6 + \left(6y_t^2 + 2\,\mathrm{Tr}(f^\dagger f) - \frac{15}{2}g'^2 - \frac{9}{2}g^2\right)\lambda_5 + 3g'^4, \tag{B5}$$

$$\kappa\beta_{\lambda_6} = 4(\lambda_2 + \lambda_3 + \lambda_6)\lambda_6 + 4\lambda_4\lambda_5 + (2\,\mathrm{Tr}(f^\dagger f) - 6g'^2 - 6g_X^2)\lambda_6. \tag{B6}$$

The beta functions for the top Yukawa coupling and the lepton Yukawa couplings to the charged scalar are

$$\kappa\beta_{y_t} = y_t\left(\frac{9}{2}y_t^2 - 8g_3^2 - \frac{9}{4}g^2 - \frac{17}{12}g'^2\right), \tag{B7}$$

$$\kappa\beta_{f_{ij}} = 4(ff^\dagger f)_{ij} + f_{ij}\left(4\,\mathrm{Tr}(f^\dagger f) - \frac{9}{2}g^2 - \frac{3}{2}g'^2\right). \tag{B8}$$

Here, we have ignored the charged lepton Yukawa couplings to the SM Higgs field. When a single lepton coupling to the charged scalar, e.g., $f \equiv |f_{12}|$, is dominant, the RG equation for that becomes

$$\kappa\beta_f = f\left(12f^2 - \frac{9}{2}g^2 - \frac{3}{2}g'^2\right). \tag{B9}$$

The beta functions for the gauge couplings are

$$\kappa\beta_{g'} = \frac{43}{6}g'^3, \qquad \kappa\beta_g = -\frac{19}{6}g^3, \qquad \kappa\beta_{g_3} = -7g_3^3, \qquad \kappa\beta_{g_X} = \frac{1}{3}g_X^3. \tag{B10}$$

[1] G. Jungman, M. Kamionkowski, and K. Griest, Phys. Rep. **267**, 195 (1996); C. Munoz, Int. J. Mod. Phys. A **19**, 3093 (2004).
[2] T. Bringmann, X. Huang, A. Ibarra, S. Vogl, and C. Weniger, J. Cosmol. Astropart. Phys. 07 (2012) 054.
[3] C. Weniger, J. Cosmol. Astropart. Phys. 08 (2012) 007.
[4] E. Tempel, A. Hektor, and M. Raidal, J. Cosmol. Astropart. Phys. 09 (2012) 032; 11(2012), A01.
[5] M. Su and D. P. Finkbeiner, arXiv:1206.1616.
[6] E. Bloom *et al.* (Fermi-LAT Collaboration), arXiv:1303.2733.
[7] F. Aharonian, D. Khangulyan, and D. Malyshev, arXiv:1207.0458.
[8] M. Su, T. R. Slatyer, and D. P. Finkbeiner, Astrophys. J. **724**, 1044 (2010).
[9] S. Profumo and T. Linden, J. Cosmol. Astropart. Phys. 07 (2012) 011.
[10] D. Whiteson, J. Cosmol. Astropart. Phys. 11 (2012) 008.
[11] D. P. Finkbeiner, M. Su, and C. Weniger, J. Cosmol. Astropart. Phys. 01 (2013) 029.
[12] D. Whiteson, arXiv:1302.0427.
[13] A. Hektor, M. Raidal, and E. Tempel, arXiv:1209.4548.
[14] M. Ackermann *et al.* (LAT Collaboration), Phys. Rev. D **86**, 022002 (2012).
[15] A. Abramowski *et al.* (H.E.S.S. Collaboration), Phys. Rev. Lett. **110**, 041301 (2013).
[16] J. M. Cline, Phys. Rev. D **86**, 015016 (2012).
[17] K.-Y. Choi and O. Seto, Phys. Rev. D **86**, 043515 (2012); **86**, 089904(E) (2012).
[18] S. Tulin, H.-B. Yu, and K. M. Zurek, Phys. Rev. D **87**, 036011 (2013).
[19] H. M. Lee, M. Park, and W.-I. Park, Phys. Rev. D **86**, 103502 (2012); H. M. Lee, M. Park, and W.-I. Park, J. High Energy Phys. 12 (2012) 037; H. M. Lee, M. Park, and V. Sanz, J. High Energy Phys. 03 (2013) 052; D. Das, U. Ellwanger, and P. Mitropoulos, J. Cosmol. Astropart. Phys. 08 (2012) 003; K. Schmidt-Hoberg,

F. Staub, and M. W. Winkler, J. High Energy Phys. 01 (2013) 124.
[20] E. Dudas, Y. Mambrini, S. Pokorski, and A. Romagnoni, J. High Energy Phys. 08 (2009) 014; Y. Mambrini, J. Cosmol. Astropart. Phys. 12 (2009) 005; E. Dudas, Y. Mambrini, S. Pokorski, and A. Romagnoni, J. High Energy Phys. 10 (2012) 123; C. B. Jackson, G. Servant, G. Shaughnessy, T. M. P. Tait, and M. Taoso, J. Cosmol. Astropart. Phys. 04 (2010) 004; arXiv:1302.1802; arXiv:1303.4717.
[21] S. Kanemura, S. Matsumoto, T. Nabeshima, and N. Okada, Phys. Rev. D **82**, 055026 (2010).
[22] O. Lebedev, H. M. Lee, and Y. Mambrini, Phys. Lett. B **707**, 570 (2012); A. Djouadi, O. Lebedev, Y. Mambrini, and J. Quevillon, Phys. Lett. B **709**, 65 (2012).
[23] Y. Farzan and A. R. Akbarieh, arXiv:1211.4685.
[24] T. Abe, M. Kakizaki, S. Matsumoto, and O. Seto, Phys. Lett. B **713**, 211 (2012).
[25] S. Baek, P. Ko, W.-I. Park, and E. Senaha, J. High Energy Phys. 05 (2013) 036.
[26] L. Wang and X.-F. Han, Phys. Rev. D **87**, 015015 (2013).
[27] E. J. Chun, H. M. Lee, and P. Sharma, J. High Energy Phys. 11 (2012) 106.
[28] K. Kannike, Eur. Phys. J. C **72**, 2093 (2012).
[29] E. W. Kolb and M. S. Turner, *The Early Universe* (Addison-Wesley, Reading, MA, 1990).
[30] P. Gondolo and G. Gelmini, Nucl. Phys. **B360**, 145 (1991).
[31] W. Buchmuller and M. Garny, J. Cosmol. Astropart. Phys. 08 (2012) 035.
[32] T. Cohen, M. Lisanti, T. R. Slatyer, and J. G. Wacker, J. High Energy Phys. 10 (2012) 134.
[33] M. Asano, T. Bringmann, G. Sigl, and M. Vollmann, Phys. Rev. D **87**, 103509 (2013).
[34] K. Griest and D. Seckel, Phys. Rev. D **43**, 3191 (1991).
[35] J. Fan and M. Reece, arXiv:1301.2597.
[36] ATLAS Collaboration, Report No. ATLAS-CONF-2013-012; CMS Collaboration, Report No. CMS-HIG-13-001.
[37] J. Baglio, A. Djouadi, and R. M. Godbole, Phys. Lett. B **716**, 203 (2012).
[38] J. R. Espinosa, C. Grojean, M. Muhlleitner, and M. Trott, J. High Energy Phys. 12 (2012) 045.
[39] J. F. Gunion, H. E. Haber, G. Kane, and S. Dawson, *The Higgs Hunter's Guide* (Addison-Wesley, Reading, 1990).
[40] B. C. Allanach, A. Dedes, and H. K. Dreiner, Phys. Rev. D **60**, 075014 (1999); F. Ledroit and G. Sajot, Report No. GDR-S-008.
[41] D. A. Dicus, H.-J. He, and J. N. Ng, Phys. Rev. Lett. **87**, 111803 (2001); A. Ghosal, Y. Koide, and H. Fusaoka, Phys. Rev. D **64**, 053012 (2001); C. A. De Sousa Pires, and P. S. Rodrigues da Silva, Phys. Rev. D **65**, 076011 (2002); K. Cheung and O. Seto, Phys. Rev. D **69**, 113009 (2004).
[42] V. D. Barger, G. F. Giudice, and T. Han, Phys. Rev. D **40**, 2987 (1989).
[43] J. E. Kim, B. Kyae, and H. M. Lee, Phys. Lett. B **520**, 298 (2001).
[44] M. Nebot, J. F. Oliver, D. Palao, and A. Santamaria, Phys. Rev. D **77**, 093013 (2008).
[45] ATLAS collaboration, Report No. ATLAS-CONF-2012-076.
[46] CMS collaboration, Report No. CMS PAS SUS-12-022.
[47] A. Heister *et al.* (ALEPH Collaboration), Phys. Lett. B **526**, 206 (2002).
[48] A. Falkowski, F. Riva, and A. Urbano, arXiv:1303.1812; P. P. Giardino, K. Kannike, I. Masina, M. Raidal, and A. Strumia, arXiv:1303.3570.
[49] G. Degrassi, S. Di Vita, J. Elias-Miro, J. R. Espinosa, G. F. Giudice, G. Isidori, and A. Strumia, J. High Energy Phys. 08 (2012) 098.
[50] J. Elias-Miro, J. R. Espinosa, G. F. Giudice, H. M.Lee, and A. Strumia, J. High Energy Phys. 06 (2012) 031.
[51] O. Lebedev, Eur. Phys. J. C **72**, 2058 (2012).
[52] B. Batell, S. Jung, and H. M. Lee, J. High Energy Phys. 01 (2013) 135.
[53] P. A. R. Ade *et al.* (Planck Collaboration), arXiv:1303.5076.